Chinese Chemical Letters 35 (2024) 108235

Contents lists available at ScienceDirect

Chinese Chemical Letters

journal homepage: www.elsevier.com/locate/cclet

TCP-1, a novel peptide to diagnose early colon cancer

Hang Yu[a,1], Baoying Wen[a,1], Min Huang[a,1], Ru Feng[a,1], Libin Pan[a], Manyi Xu[a], Hao Lin[a], Lin Cong[a], Sen Zhang[a], Yan Li[a], Chi-Hin Cho[b,*], Chongjing Zhang[a,*], Xiaoguang Chen[a,*], Yan Wang[a,*]

[a] *State Key Laboratory of Bioactive Substances and Functions of Natural Medicines, Institute of Materia Medica, Chinese Academy of Medical Sciences, Beijing 100050, China*

[b] *School of Biomedical Sciences, Faculty of Medicine, The Chinese University of Hong Kong, Hong Kong, China*

ARTICLE INFO

Article history:
Received 18 October 2022
Revised 11 February 2023
Accepted 15 February 2023
Available online 19 February 2023

Keywords:
Colon cancer
TCP-1
Peptide
Cytokeratin 5
Pharmacokinetics/pharmacodynamics (PK/PD)

ABSTRACT

A nine cyclic peptide (TCP-1) showed excellent specificity for colon cancer. TCP-1 binds with human tumor tissues at early stages and mice tumor with diameters of 1-4 mm, suggesting that TCP-1 may be used for early diagnosis of colon cancer. The mechanism of the targeted binding of TCP-1 to colon cancer was also studied using immunoprecipitation, LC-MS and bioinformatics. After screening and identifying of the possible binding target proteins of TCP-1, keratin, type II cytoskeletal 5 was speculated to be the specific binding target protein of TCP-1 in human tumor tissue. Pharmacokinetics studies were conducted to investigate the target-mediated drug disposition of the new tumor-specific peptide by LC-MS/MS. The tissue distribution study showed that TCP-1 was found only in colon tumors (the target site) in tumor mice did not bind to any other tissues. Conjugating TCP-1 to tumor markedly increased its removal rate from blood circulation but mildly extended its staying time *in vivo*. In tumor mice, a lower AUC of TCP-1 (reduced by almost 35%) and 2-fold higher clearance were found compared to that of normal mice. The proposed metabolic pathway of TCP-1 in the kidney was also determined using LC-MS^n-IT-TOF. The high specificity and low toxicity of the peptide may be caused by its extremely tight binding to the targets. Potential applications for future clinical use, including MRI and PET/CT were also explored, and this research may promote the development of colon cancer diagnostic technology research and provide new ideas and technical routes for tumor diagnostic technology.

Colon cancer is the third most common malignancy worldwide and detecting colon cancer in a precise and early manner can ultimately improve the cure rate [1–5]. According to China's Colorectal Cancer Diagnosis and Treatment Guidelines (2020 Edition), imaging examinations can help to diagnose the stage of tumor and the remote metastasis of other organs, such as CT, MRI, and PET/CT. In addition, medical therapy should be conducted after fine baseline imaging examination, which indicates imaging diagnosis is very important for the diagnosis and treatment of colorectal cancer. In recent years, protein or peptide drugs have received considerable attention as potential diagnostic and therapeutic options. Due to the extremely tight binding of peptide drugs to their targets, these drugs exhibit high specificity and low toxicity [6–8]. We successfully applied *in vivo* phage display selection to identify the peptide CTPSPFSHC (TCP-1), which specifically recognizes colon cancer tissues [9].

The detection of tumor biomarkers and probe targets improves the early clinical diagnosis of cancer and has important clinical value for the recurrence, metastasis and prognosis of diseases. Proteomics is among the main research methods for screening tumor biomarkers and probe targets, and its experimental design focuses on differences in protein expression profiles between normal and abnormal cells or cancer and normal tissue [10]. The related protocols mainly involve a clinical sample pretreatment, such as ultrafiltration, precipitation and preliminary classification; sample separation by two-dimensional gel electrophoresis (2-DE) or liquid chromatography (LC); and different protein expression profile identification by mass spectrometry [10]. Using bioinformatics methods to retrieve the corresponding protein information and further researching the biological function of the protein of interest by immunoprecipitation and immunohistochemical methods could finally identify the target protein [11].

* Corresponding authors.
E-mail addresses: chcho@cuhk.edu.hk (C.-H. Cho), zhangchongjing@imm.ac.cn (C. Zhang), chxg@imm.ac.cn (X. Chen), wangyan@imm.ac.cn (Y. Wang).

[1] These authors contributed equally to this work.

https://doi.org/10.1016/j.cclet.2023.108235
1001-8417/

Target-mediated drug disposition (TMDD) and renal metabolism are two special features frequently observed for peptide and protein drugs but rarely occur with small-molecule drugs. TMDD refers to the interaction of a drug with its pharmacological target, which initiates the process of drug elimination. In particular, peptide and protein drugs bind to their target site with high affinity. This interaction influences the temporal profile of plasma drug concentrations. Therefore, pharmacokinetics and pharmacodynamics are no longer independent processes; instead, they become interdependent. Furthermore, even though the liver is considered to play a dominant role in the metabolism of xenobiotics, it is well established that the kidney is the major site for the metabolism of peptides [12]. In general, peptides and proteins are disadvantaged by short half-lives, which is due to rapid renal clearance. To perform metabolic characteristic studies and further develop the candidate diagnostic reagent TCP-1, it is critical to quantitate the *in vivo* and *in vitro* levels of TCP-1, which can be used to evaluate the pharmacokinetics of TCP-1 and determine the dose-effect and dose-toxicity relationship. Hence, there is a great need for reliable, accurate, and sensitive bioanalytical assays for TCP-1. However, accurately quantifying peptide-derived drugs in biological matrices remains a challenge [13,14].

Due to its high selectivity, sensitivity, and throughput, liquid chromatography tandem mass spectrometry (LC-MS/MS) is a powerful tool for qualitatively and quantitatively analyzing peptide-derived drugs in biological matrices [15–17]. Bonate *et al.* described a sensitive LC-MS/MS method for the quantification of tasidotin (ILX651), a depsipeptide [18]. Additionally, a fast and sensitive method was reported for the quantification of a novel antimicrobial peptide, SR-0379, in rats using LC-MS/MS [19]. Recently, a method of quantifying nivolumab in human plasma by LC-MS/MS was developed [20]. Indeed, LC-MS/MS has become the preferred analytical technique for the quantification of peptides.

A previous study illustrated that TCP-1 can be used to deliver fluorescein and proapoptotic peptides to tumors for imaging detection and targeted therapy [21], suggesting that TCP-1 may hold promise as an agent in diagnosis and therapy. Hence, there is a great need to further research the potential application of TCP-1.

Here, the specificity and target-mediated characteristics of TCP-1 were further evaluated using both clinical and animal tumor tissue. Moreover, TCP-1 binding site identification can reveal the molecular mechanism that explains the specificity of TCP-1 binding to colorectal tumors. Systematic pharmacokinetics studies were also investigated to determine whether TCP-1 possesses favorable PK properties with LC-MS/MS and LC-MSn-IT-TOF. Finally, the potential application of the novel candidate peptide for further clinical use in diagnosing early colorectal cancer was examined. Studying the metabolic characteristics of TCP-1 and using the targeting characteristics to find and screen potential tumor markers may provide research directions for small molecule tumor-targeting peptides, which can be used as tumor-targeting peptides for cancer diagnosis and treatment.

The structure of TCP-1, a nine cyclic peptide, is shown in Fig. 1a. The specificity identification to human colorectal tumors was first tested with 137 clinical colorectal tissue samples, including 91 tumor, 21 adenomas, 13 polyps, 4 adjacent tissues to carcinoma, and 8 normal mucosae. The human tissue was collected from No. 7 Medical Center, PLA General Hospital, and the clinical study was approved by the Ethics Committee (approval No. 2013-11) of No. 7 Medical Center, PLA General Hospital and informed consent was obtained from the subjects. As shown in Fig. 1b and Fig. S1a (Supporting information), biotin-conjugated TCP-1 (Bio-TCP-1) and biotin-control peptide (Bio-Control) were incubated with human colorectal tissue cryosections, and were subjected to anti-CD31 detection. Immunofluorescence staining showed that TCP-1 colocalized with CD31 in human tumor tissue but did not show fluorescence in normal colorectal tissue. The biotin-control peptide showed no fluorescence in either human tumor tissue or normal tissue.

A total of 64.84% (59/91) of colorectal adenocarcinomas from a total of 91 patents were recognized by TCP-1 (Fig. 1c). Positive binding was found in tumor tissues at more early stages. For 59 colorectal tumor samples with exact clinical stage, the total positive binding rate of TCP-1 was 64.41% (38/59), among which the clinical II stage colorectal cancer targeted positive rate was 92.31% (12/13) and the positive binding rate to both clinical I and II stage colorectal cancer was 86.36% (19/22) (Fig. 1e).

The TNM staging system is among the most common malignant tumor staging systems. For T staging, which represents the degree of primary tumor invasion, the positive binding rates to T2, T3 and T4 stage were 62.50% (10/16), 63.64% (21/33) and 66.67% (6/9), respectively. For N staging, which indicates regional lymph node metastasis, the TCP-1-targeted positive rate to N0 stage was 86.36% (19/22). For M staging, which represents distant metastasis, the TCP-1-targeted positive rate to the M0 stage was 64.81% (35/54) (Fig. 1f). The specificity of TCP-1 for human precancerous lesions was also detected. For 24 pathological colorectal lesion samples, including 21 adenomas and 3 polyps, the positive binding rate to high-level intraepithelial neoplasia tissue samples was 66.67% (2/3). In addition, TCP-1 did not interact with the 2 inflammatory polyp samples collected (Fig. 1d).

The specificity of TCP-1 for mouse colorectal tumors was also studied. All research was conducted in accordance with the institutional guidelines and ethics and approved by the Laboratories Institutional Animal Care and Use Committee of the Chinese Academy of Medical Sciences and Peking Union Medical College (No. 00003545). TCP-1 colocalized with CD31 in mouse tumors but did not show fluorescence in normal tissue (Fig. 2a). Since tumor size can represent tumor progression, TCP-1 was bound to mouse tumors with different diameters. For 21 colorectal tumors collected, the total positive binding rate was 61.90% (13/21), among which the tumor size within 1-4 mm targeted positive rate was 85.71% (6/7) (Fig. 2b), which indicated that TCP-1 tended to bind to early-stage tumors. Then, FITC-TCP-1 was intravenously injected into tumor-bearing mice, and various tissues were collected. As shown in Fig. 2c, FITC-TCP-1 localized in the tumor tissues but was not detectable in control organs, which suggested that TCP-1 specifically targeted tumor tissues but not other control organs. Next, the proteins bound to TCP-1 were identified (Fig. 2d). The cell membrane proteins of colon 26 were extracted, immunoprecipitation was conducted, and the protein concentration gradually decreased after interaction with TCP-1 (Table S1 in Supporting information). Next, both Bio-Control miscellaneous protein and Bio-TCP-1 target protein were separated using SDS-PAGE. As shown in Fig. 2e, Bio-TCP-1-target protein exhibited protein bands in the vicinity of 95-72, 72, 55 and 34-26 kDa, while Bio-Control-miscellaneous protein showed a light protein band in the vicinity of 72 kDa. The target protein was identified by mass spectrometry. The results are shown in Tables S2-S6 (Supporting information). All proteins shown in the tables were confirmed to be expressed in both mice and humans.

Among them, 3 candidates (keratin, type II cytoskeletal 5, keratin, type II cytoskeletal 2 epidermal, keratin, type II cytoskeletal 1) are most likely to be the specific binding site of TCP-1 (Table S7 in Supporting information), considering that the top three proteins were in each protein band and mainly based on the correlation between the candidate proteins and colon cancer development. Then, the binding site of TCP-1 was validated by a peptide overlay assay. As shown in Fig. 2f, cytokeratin 5 colocalized with Bio-TCP-1 and CD31, while cytokeratin 1 and cytokeratin 2 did not show fluorescence in the human tumors. Thus, we speculated that the binding site of TCP-1 was keratin, type II cytoskeletal 5.

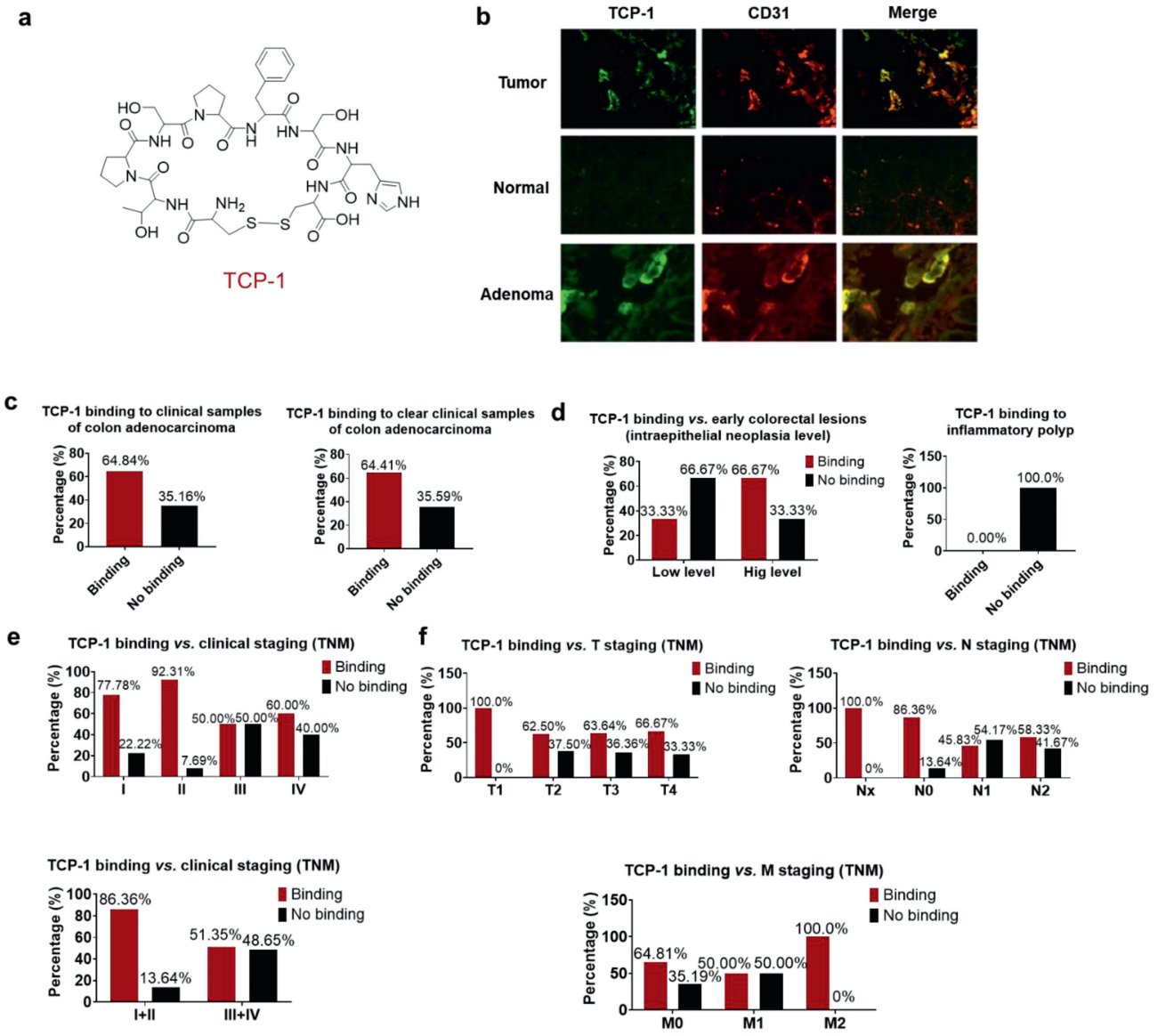

Fig. 1. TCP-1-specific targeting of human colon tumor tissue. (a) Structures of cyclic peptide TCP-1. (b) Immunofluorescence staining of human colorectal tissue with TCP-1. (c) The total positive rate of TCP-1 targeting human colon tumors (left) and binding to colon tumor samples with clear clinical stage (right). (d) Positive rate of TCP-1 binding to colorectal tissues of different grades of intraepithelial neoplasia (left) and inflammatory polyps (right). (e) Positive rate of TCP-1 binding to colon tumor tissues of different clinical stages (above) and binding to colorectal tumors of clinical stages I and II, III and IV (below). (f) Positive rate of TCP-1 binding to T stage (upper left), N stage (upper right) and M stage (below).

Furthermore, the pharmacokinetic characteristics of TCP-1 were studied. A highly sensitive method for quantitating TCP-1 was established by LC-MS/MS, and corresponding methodology validation was conducted (Tables S8-S10 in Supporting information). Three dose groups (12.5, 25, and 50 mg/kg) were studied in normal mice and tumor-bearing mice. The TCP-1 plasma pharmacokinetic profiles are presented in Fig. 3a. A two-compartment model best fit the plasma TCP-1 concentrations versus time data, and the pharmacokinetic parameters associated with that model are presented in Table S11 (Supporting information). The plasma concentrations of TCP-1 in the three groups decreased rapidly and were undetectable beyond 360 min after TCP-1 administration. The maximum plasma concentration (C_{max}) ratios and the area under the plasma concentration-time curve from zero to the time of the last quantifiable concentration ($AUC_{(0\text{-}t)}$) ratios increased proportionally as the dose increased (1:2:4), as shown in Figs. S2a-c (Supporting information); this result provided evidence supporting the linear plasma pharmacokinetics of TCP-1. No significant difference was observed between the pharmacokinetic parameters of TCP-1 in the two species of normal mice, which indicated that the plasma pharmacokinetics of TCP-1 were not difference among rodent species. However, the plasma TCP-1 concentration *versus* time profile in tumor mice moved left (Fig. 3a). While no significant difference was observed between the C_{max} of TCP-1 in tumor mice and normal mice, a significant difference in $t_{1/2}$, AUC, CL and Vz was observed (Fig. S2d in Supporting information). With three different doses of TCP-1, a lower exposure for TCP-1 in tumor mice was observed compared to TCP-1 in normal ICR and Balb/c mice. Lower $AUC_{(0\text{-}\infty)}$ values of 358.42 ± 33.58, 530.19 ± 94.51, and 1152.11 ± 184.58 μg mL^{-1} min and $AUC_{(0\text{-}t)}$ values of 357.96 ± 34.35, 529.77 ± 94.05, and 1151.91 ± 184.46 μg mL^{-1} min were found following the administration of various TCP-1 doses ranging from 12.5 mg/kg to 50 mg/kg, suggesting a reduction of almost 35% compared with that of normal mice (Fig. 3b and Fig. S2d). In normal mice, the terminal half-life of TCP-1 was approximately 0.5 h, the volume of distribution was approximately 1200 mL/kg, and the clearance was

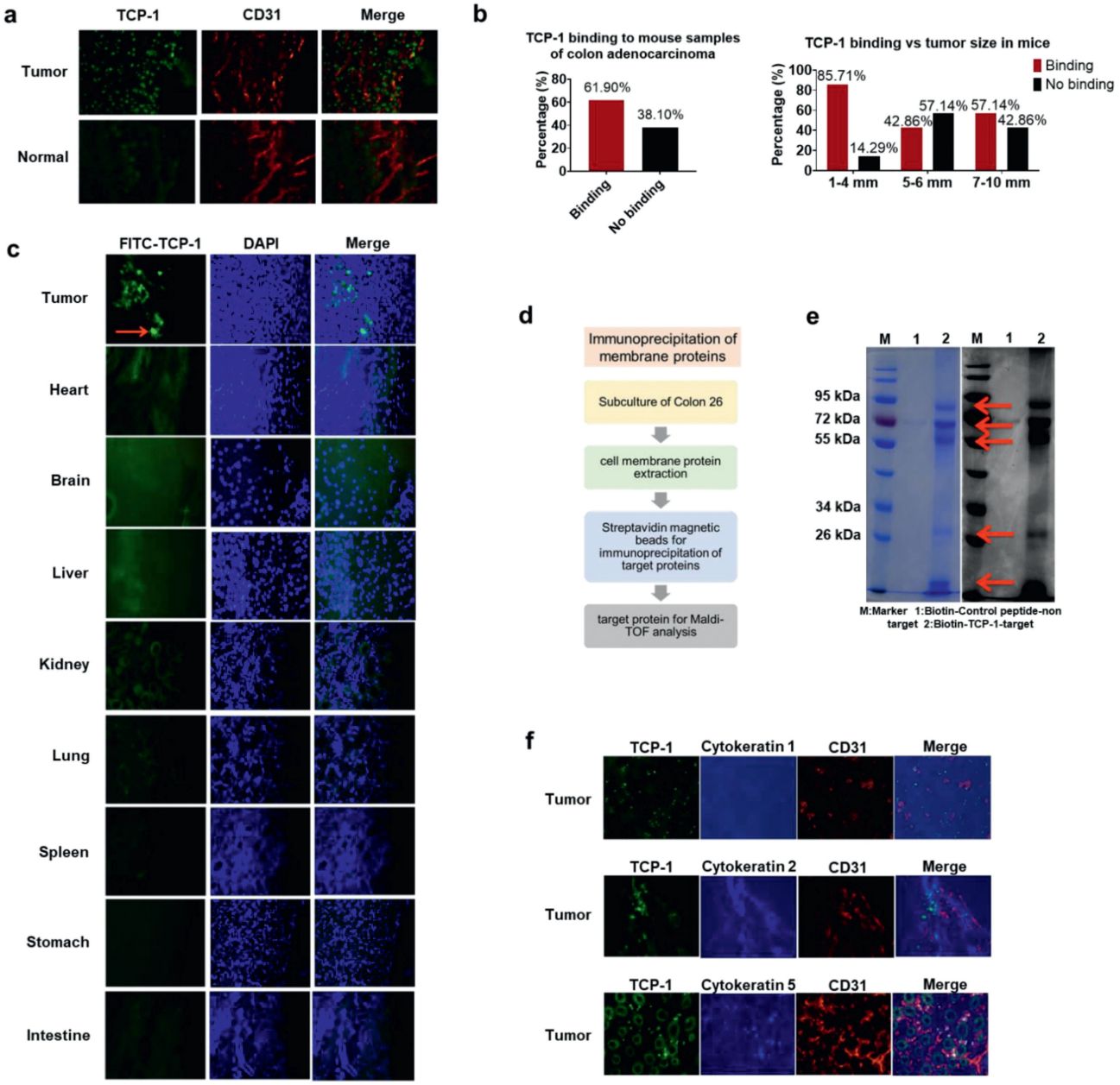

Fig. 2. Identification of TCP-1 binding sites. (a) Immunofluorescence staining of the colorectal tissue of mice with TCP-1. (b) The total positive rate of TCP-1 targeting colon tumors in mice (left) and binding to colon tumor tissues of mice with different diameters (right). (c) Tissue imaging of FITC-TCP-1 injected into tumor mice. (d) Scheme showing the identification of TCP-1 binding sites. (e) Results of the biotin-TCP-1-target protein complex. (f) Immunofluorescence staining of human colon cancer with anti-cytokeratin 1, anti-cytokeratin 2 and anti-cytokeratin 5.

rapid (approximately 25 mL min^{-1} kg^{-1}). However, the presence of peptide in the body was extended when the TCP-1 was conjugated to tumors, which led to an increase in $t_{1/2}$. The conjugation of TCP-1 to tumors also resulted in a marked increase in the rate of peptide removal from the blood circulation, which is reflected in the reduced plasma AUC and increased clearance (45 mL min^{-1} kg^{-1}) and volume of distribution (2500 mL/kg) (Fig. S2d).

The tissue distribution of TCP-1 was determined to study the high affinity of TCP-1 for the targets. In normal mice, TCP-1 did not bind to any tissues. In tumor mice, higher concentrations with all 3 dosing forms of TCP-1 were only reached in tumors within 0.5 h (the earliest time point for sampling) and reached peak concentrations (in a dose-dependent manner) in 1 h (Fig. 3c). Analysis of other tissues (liver, spleen, kidney, lung, heart, muscle, *etc.*) showed that TCP-1 did not bind these tissues (Fig. 3c), which indicated that TCP-1 exhibits good tissue specificity. The excretion characteristics of TCP were then studied. TCP-1 was rapidly excreted through urine, mainly in its prototype form. As shown in Figs. S4c and d (Supporting information), most of the TCP-1 (>50%) was excreted during the first 1 h after administration in mice. Urinary cumulative excretions of TCP-1 are depicted in Fig. 3d. Following the administration of various TCP-1 doses ranging from 12.5 to 50 mg/kg, the total recovery of TCP-1 in urine was 55.55% ± 14.49%, 53.54% ± 2.32%, 60.29% ± 17.83% in ICR mice, 52.58% ± 14.80%, 56.92% ± 10.89%, 59.04% ± 13.78% in Balb/c mice, and 53.34% ± 8.25%, 64.61% ± 13.48% and 60.28% ± 18.39% in tumor mice. The urinary cumulative excretion of TCP-1 was increased in proportion to the dose increase, as shown in Fig. 3d. Therefore, the short half-life of this peptide may be due to its rapid renal clearance. In urine excretion, the total recovery of TCP-1 in urine

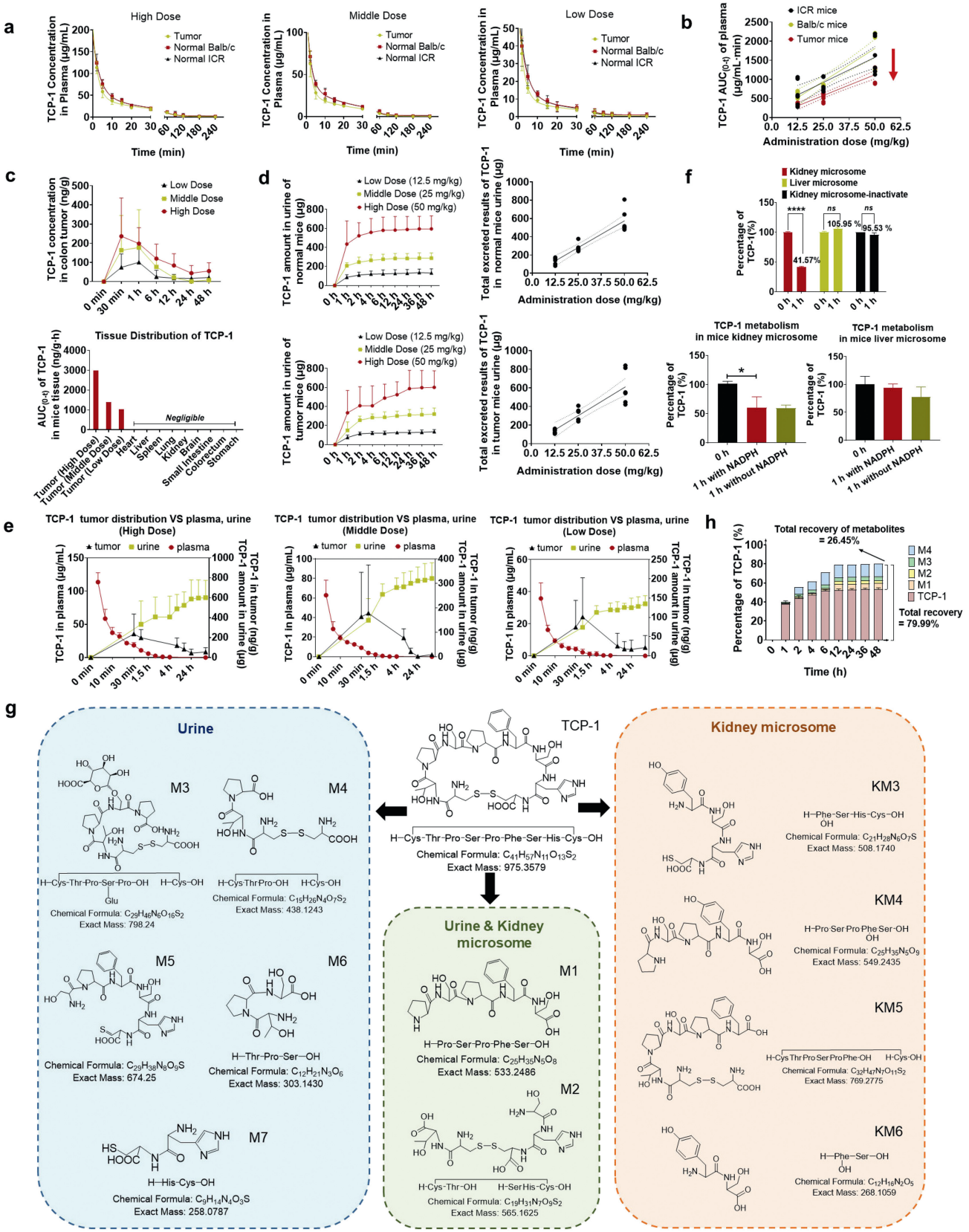

Fig. 3. Pharmacokinetic studies of TCP-1. (a) The plasma concentration-time curve of TCP-1 comparison between normal mice and tumor mice. (b) Comparison of the correlation of $AUC_{(0\text{-}t)}$ with dosage between normal mice and tumor mice. (c) TCP-1 concentration in colon tumors (above) and tissue distribution of TCP-1 (below). (d) Cumulative excretions of TCP-1 by urine 48 h after i.v. administration in normal mice (above left) and tumor mice (below left); and cumulative excretions of TCP-1 *versus* dosage in normal mice (above right) and tumor mice (below right). (e) TCP-1 tumor distribution *versus* plasma and urine (12,5, 25.0 or 50.0 mg/kg; Data are mean ± S.D., $n = 6$ per group). (f) Metabolism of TCP-1 incubated with mouse kidney and liver microsomes. $^{****}P < 0.0001$; *ns,* no significance. (g) Proposed metabolic pathway of TCP-1 *in vivo* and *in vitro*. (h) Recovery of TCP-1 and its metabolites obtained from mouse urine (Data are mean ± S.D., $n = 3$ per group).

showed no significant difference between normal mice and the tumor model (Fig. S4e in Supporting information). Less TCP-1 was excreted in the first hour, and a significant difference was observed between the cumulative excretions in 2-48 h of TCP-1 in tumor mice and normal mice (Fig. S4f in Supporting information). More TCP-1 tends to be excreted after 2 h in tumor mice, suggesting that the interaction of TCP-1 with tumors extended its staying time in the body. TCP-1 binding to the target site may slow its excretion rate and is the limiting step in its elimination. The abundance of TCP-1 in tumors was compared with that in plasma and urine within 48 h (Fig. 3e). In summary, in the three dose groups in tumor mice, TCP-1 decreased rapidly from the blood within 30 min and then conjugated to the tumor; as a result, the peptide reached its peak concentrations in 1 h. After the peptides and targets finished binding, TCP-1 was eliminated from urine, and the vast majority accumulated within 2 h. Plasma elimination, tumor distribution and urine excretion are closely continuous processes.

The *in vitro* metabolism assays for TCP-1 showed that a significant reduction in TCP-1 occurred in kidney but not liver microsomes independent of NADPH (Fig. 3f, Figs. S3a and b in Supporting information). No significant decrease in TCP-1 occurred in inactive kidney fractions (Fig. 3f). We also evaluated the roles of enzymes (FMOs, CYP450, metalloproteinase, serine proteinase, and reductase) in the metabolism of TCP-1 (Figs. S3c-g in Supporting information). It seemed that metalloproteinase, serine proteinase and reductase may be involved in the renal metabolism of TCP-1. After TCP-1 was intravenously injected in mice, metabolites were observed only in the urine and not in the plasma or feces. The extracted-ion chromatogram for the TCP-1 metabolites in urine is shown in Fig. S4a (Supporting information), and the extracted-ion chromatogram of the TCP-1 metabolites detected in the mouse kidney microsome incubation system is shown in Fig. S4b (Supporting information). The major metabolites were identified using the accurate molecular weight data observed in the MS^n spectra obtained with LC/MS^n-IT-TOF. The metabolites found *in vivo* in mouse urine and *in vitro* in kidney microsomes are shown in Table S12 (Supporting information), along with the retention times, chemical composition, and characteristic fragments. At least seven potential metabolite peaks were detected in urine using IT-TOF, including **M1**, **M2**, **M3**, **M4**, **M5**, **M6** and **M7**, and six potential metabolite peaks were detected in kidney microsomes (**M1**, **M2**, **KM3**, **KM4**, **KM5** and **KM6**). These results showed that two of the same metabolites (**M1** and **M2**) were detected in urine and kidney microsomes. All potential metabolites were more polar than TCP-1, and the proposed structures, which are displayed in Fig. 3g, were consistent with metabolism by hydrolysis of the cyclopeptide or hydroxylation of the aromatic ring of the amino acid. Based on the chromatogram, the metabolites consistent with peptide linkage hydrolysis were most prevalent in mouse urine. The metabolites consistent with both peptide linkage hydrolysis and hydroxylation of the aromatic ring were most prevalent in mouse kidney microsomes. Following the intravenous administration of 25.0 mg/kg TCP-1, 26.45% of TCP-1 was recovered as metabolites, and the total recovery of TCP-1 (including the prototype compound and the major metabolites) in urine was 79.99% (Fig. 3h).

Next, potential applications for the clinical diagnostic imaging of TCP were explored. Gd-TCP-1 was used to study the potential application of TCP-1 for MRI. As shown in Fig. 4a, 8 min after the tail vein injection of Gd-DTPA (1 mmol/kg), a magnetic resonance contrast agent, angiographic enhancement in the area with rich blood flow can be observed, and there was also a certain blood flow enhancement around the rectal cavity, and the enhancement was weakened after 30 min. In addition, 8 min after the tail vein injection of Gd-conjugated TCP-1 (Gd-TCP-1) (240 μmol/kg), contrast enhancement of the tissue around the rectal cavity was observed. Since the injected dose of Gd-TCP-1 was equivalent to 1/5 of the Gd-DTPA, the potential application of Gd-TCP-1 on MRI was preliminarily confirmed at the level of small animal imaging.

Then, radiolabeled ^{18}FAl-NOTA-TCP-1 was introduced to evaluate the potential application of TCP-1 for PET/CT. $^{18}F^-$ was produced from an HM-20 medical cyclotron. The synthetic procedure of ^{18}FAl-NOTA-TCP-1 is presented in Section 1.23 of Supporting information. The *in vitro* stability of ^{18}FAl-NOTA-TCP-1 was determined with radio-HPLC. The radiopharmaceutical study showed excellent stability *in vitro*, including in saline, 5% HSA, and mouse whole blood, which remained almost intact for up to 4 h (Figs. S5a-c in Supporting information). The partition coefficient of ^{18}FAl-NOTA-TCP-1 was calculated as $\log D_{7.4} = -2.53 \pm 0.09$, with the majority of radioactivity concentrated in the water phase (>98%), indicating the superior hydrophilicity of ^{18}FAl-NOTA-TCP-1.

As shown in Fig. 4b, in colon 26 cells, the highest uptake of ^{18}FAl-NOTA-TCP-1 was observed at 60 min (1.09 ± 0.09 AD%), which could be blocked by adding excess nonradiolabeled precursor (0.72 ± 0.05 AD%), indicating the specific binding between ^{18}FAl-NOTA-TCP-1 and colon 26 cells. The uptake of ^{18}FAl-NOTA-TCP-1 in colon 26 cells decreased from 60 min to 120 min.

Furthermore, a pharmacokinetics study of ^{18}FAl-NOTA-TCP-1 in mice provided conclusive evidence for its rapid clearance from the body. As shown in Figs. 4c and d, the pharmacokinetics of ^{18}FAl-NOTA-TCP-1 followed two-phase decay in normal mice (Fig. 4c) and tumor mice (Fig. 4d), with extremely short biodistribution half-lives of only 2.75 min and 1.31 min, respectively, which corresponded to the rapid distribution of TCP-1 to tumors. With further optimization, TCP-1 was expected to be used in PET/CT.

In this study, we successfully applied the immunofluorescent staining approach to identify the specificity of the peptide CTP-SPFSHC (TCP-1) to mouse and human colorectal tumors. TCP-1 can specifically bind to human and mouse colon tumor blood vessels. Through the statistics of the positive rate of TCP-1 targeted binding, it was found that for 59 colorectal tumors of different clinical stages, the total positive rate of TCP-1 binding was 64.41%, of which the targeted positive rate of clinical stage I and II colorectal cancer was 86.36%. In 21 mouse colon cancer tumor tissues, the positive rate of TCP-1 targeting was 61.90%, and 85.71% targeted tumors with diameters within 1-4 mm. *In vivo* experiments also demonstrated that FITC-TCP-1 could specifically recognize colorectal tumors in tumor-bearing mice after injection into the tail vein, suggesting that TCP-1 may be used for the early diagnosis of colon cancer.

It is possible to discover new tumor markers and important signaling pathways through the binding site of the TCP-1 polypeptide. We attempted to isolate the receptor molecules bound by TCP-1 using the pull-down technique. Since tumor tissue contains a variety of cellular interference components and TCP-1 can well identify colon 26 cells, of which the protein composition is relatively simple, we incubated Biotin-TCP-1 with the cell lysate to separate the binding molecules. Based on the high-affinity binding between biotin and avidin, we used streptavidin magnetic beads to perform protein precipitation with colon 26 cell membrane proteins. Blank magnetic beads and Biotin-Control peptide-magnetic bead complex were used to remove impurities for the proteins bound to avidin and disulfide bonds, and then a relatively high purity Biotin-TCP-1-Target protein complex was obtained. Finally, the target protein was isolated and identified by LC/MS-MALDI-TOF. The peptide information, protein amount, and protein-specific peptides identified by MALDI-TOF were combined to match the membrane protein database of Balb/c mouse colorectal cancer cells. After combining the correlation between carcinogenesis and development, we screened potential target proteins according to the matching score that were expressed in both mice and humans. To confirm the accuracy of the target of TCP-1 identified by immunoprecipitation, further study will be continued in the future on the proteins ex-

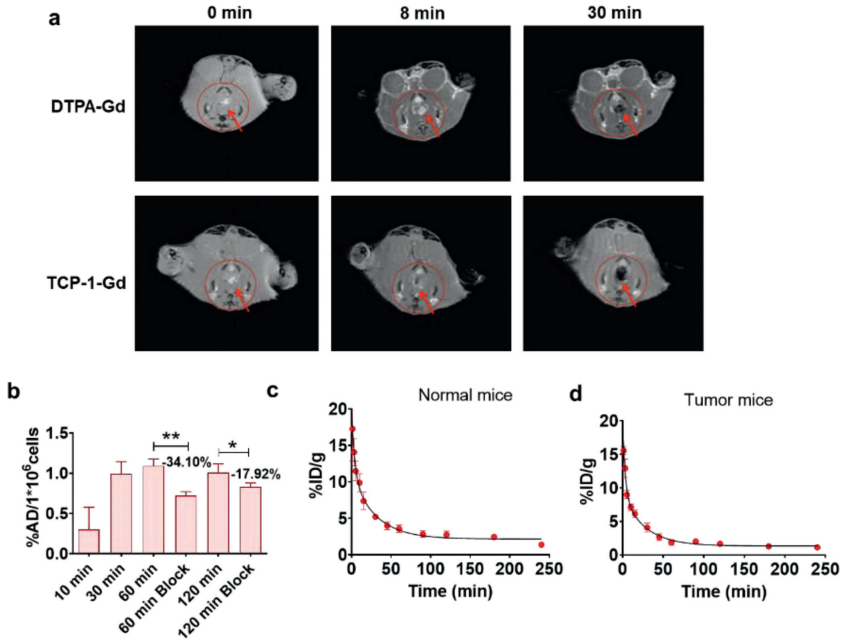

Fig. 4. Potential application for TCP-1. (a) Magnetic resonance imaging of tumor mice after administration of Gd-TCP-1. (b) Tracer uptake in colon 26 cells at different time points after the addition of ^{18}FAl-NOTA-TCP-1 (74 kBq) (Data are mean ± S.D., $n = 3$ per group). Pharmacokinetic study of ^{18}FAl-NOTA-TCP-1 in (c) normal mice and (d) tumor mice (Data are mean ± S.D., $n = 3$ per group). $^{*}P < 0.05$, $^{**}P < 0.01$.

tracted from human colon tumor tissue and from mouse normal intestinal mucosal cells. As a result, the 3 most likely proteins were screened from the potential target protein group, and then the candidate target proteins were verified by *in vitro* immunofluorescence staining. Cytokeratin 5 can colocalize with TCP-1 and CD31 at the same time, while Cytokeratin 1, Cytokeratin 2 fail in human tumor tissue. It has been reported that the expression of keratin, type II cytoskeletal 5 (Cytokeratin 5) is upregulated in the tumor tissue of patients. Immunohistochemical data showed that KRT5 is significantly stained in tumor areas compared to normal tissue areas [22]. In another study, 30 poorly differentiated adenocarcinoma samples exhibited expression of Cytokeratin 5 and p63, compared with tubular, tubular-villous, and villous adenomas, which could be related to divergent differentiation during the development of colorectal cancer [23].

At the same time, considering the fact that the positive rate of TCP-1 targeting clinical phase II was as high as 92.31%, we speculated that the target protein specifically bound by TCP-1 was likely Cytokeratin 5. To further confirm the target protein specifically bound by TCP-1, we will further expand the sample size. KRT5 knockout mice or cells will be used for further confirmation. Since cytokeratin 19 (Cyfra21-1) is already used in the clinic as a protein tumor marker [24], the identified possible target protein, keratin, type II cytoskeletal 5, might be a biomarker for colon cancer progression.

The pharmacokinetics and metabolism of TCP-1 in both normal mice and tumor mice were also characterized, and the peptide TCP-1 suffered from short half-lives due to rapid renal clearance. Following the administration of various doses ranging from 12.5 mg/kg to 50 mg/kg, the area under the plasma concentration-time curve from zero to the time of the last quantifiable concentration ($AUC_{(0\text{-}t)}$) ratios increased proportionally as the dose increased, which demonstrated that TCP-1 was not stored in the body. TCP-1 was relatively stable in the plasma and liver, and the kidney was the main excretion and metabolism organ of TCP-1. The metabolic capacity of the kidney is important for exogenously administered peptide or protein drugs such as TCP-1, resulting in its activation or inactivation, disposition and elimination. Nonspecific proteolysis is considered a major elimination pathway for the peptide *in vivo*. The metabolites consistent with both peptide linkage hydrolysis and hydroxylation of the aromatic ring may only occur *in vitro*. Dramatic differences in TCP-1 pharmacokinetics between normal mice and tumor mice were found. As pharmacokinetics (PK) methods were conducted, TCP-1 appeared to show good penetration into the tumor after intravenous administration. In normal mice, TCP-1 was rapidly eliminated from plasma (elimination half-life of 0.5 h), but no TCP-1 was detected in the liver, spleen, kidney, lung, heart, muscle, *etc*. When TCP-1 was administered to tumor mice, TCP-1 likely accumulated in the tumor (The peak concentrations were 100.36, 181.93 and 239.00 ng/g following the administration of various doses ranging from 12.5 mg/kg to 50 mg/kg.). This interaction influenced the profile of plasma drug concentrations. TCP-1 was eliminated more slowly when conjugated to the tumor (longer $t_{1/2}$). Therefore, a remarkably lower exposure of TCP-1 in the blood circulation was observed, which was reflected in the reduced plasma AUC (a reduction in almost 35% compared to that of normal mice) and increased clearance and volume of distribution (approximately 2-fold more compared to that of normal mice). TCP-1 binding to the target site may also extend its time in the body and slow its excretion rate. The higher the dose of TCP-1 treatment, the more obvious the significant difference between the cumulative excretions in 2-48 h of TCP-1 in tumor mice and normal mice, which could be explained by the target-mediated drug disposition of the peptide TCP-1. The results indicated that the high specificity and low toxicity of peptide drugs may derive from their extremely tight binding to their targets, and the interaction influenced their pharmacokinetic characteristics.

The potential applications of TCP-1 in the early diagnosis of colorectal cancer were also explored. The coupling of TCP-1 and gadolinium was used for nuclear magnetic resonance imaging of tumor mice to observe whether the specific binding of TCP-1 to colon tumors produced an enhancement in tumor site angiography. The results of self-control experiments in tumor mice showed that Gd-TCP-1 equivalent to 1/5 of the contrast agent Gd-DTPA dose exhibited a certain contrast enhancement in tumor tissue around the intestinal lumen. Further studies will be conducted by select-

ing a positive contrast agent with a better contrast enhancement effect to couple with TCP-1 to verify the application of TCP-1 on MRI. We also designed and synthesized NOTA-TCP-1. After labeling ^{18}F, ^{18}FAl-NOTA-TCP-1 showed good stability in saline, 5% HAS, and whole mouse blood *in vitro* for 4 h. The lipid-water partition coefficient showed strong water solubility. The high uptake of ^{18}FAl-NOTA-TCP-1 was observed when coincubated with colon 26 cells, which indicated a high potential for application to PET/CT *in vivo* in the future.

In conclusion, a nine cyclic peptide (TCP-1) showed excellent specificity for blood vessels in early-stage human and mouse colon tumors with diameters as small as 1-4 mm. The target protein specifically bound by TCP-1 was probably keratin, type II cytoskeletal 5. Pharmacokinetics studies showed that the conjugation of TCP-1 to tumors markedly increased its removal rate from blood circulation but mildly extended its presence *in vivo*. Peptides with high specificity and low toxicity may be applied for MRI and PET/CT for clinical use in the future, which may promote the development of colon cancer diagnostic technology research and provide new ideas and technical routes for tumor diagnostic technology.

Declaration of competing interest

The authors declare that they have no known competing financial interests or personal relationships that could have appeared to influence the work reported in this paper.

Acknowledgments

The authors thank Dr. Xiaoxiao Yang (Institute of Materia Medica, Chinese Academy of Medical Sciences) for the contributions to this work. This project was supported by the CAMS Innovation Fund for Medical Sciences (CIFMS, No. 2021-I2M-1-027), National Natural Science Foundation of China (Nos. T2192972, 81402997), Key Project of Beijing Natural Science Foundation (No. 7181007), National High-tech Research and Development Plan (863 Plan, No. 2014AA020803) and Beijing Key Laboratory of Non-Clinical Drug Metabolism and PK/PD Study (No. Z141102004414062). We would like to thank Shimadzu (China) Co., Ltd. for technological support.

Supplementary materials

Supplementary material associated with this article can be found, in the online version, at doi:10.1016/j.cclet.2023.108235.

References

[1] M. Arnold, M.S. Sierra, M. Laversanne, et al., Gut 66 (2017) 683-669.
[2] L.A. Torre, F. Bray, R.L. Siegel, et al., CA Cancer J. Clin. 65 (2015) 87–108.
[3] H. Sung, J. Ferlay, R.L. Siegel, et al., CA Cancer J. Clin. 71 (2021) 209–249.
[4] M.M. Fidler, F. Bray, I. Soerjomataram, Scand. J. Public Health 46 (2018) 27–36.
[5] M.M. Fidler, F. Bray, S. Vaccarella, I. Soerjomataram, Int. J. Cancer 140 (2017) 2709–2715.
[6] K. Jin, Future Med. Chem. 12 (2020) 1687–1690.
[7] A. Varanko, S. Saha, A. Chilkoti, Adv. Drug. Deliv. Rev. 156 (2020) 133–187.
[8] E. Fisher, K. Pavlenko, A. Vlasov, G. Ramenskaya, Pharmaceut. Med. 33 (2019) 9–20.
[9] Z.J. Li, W.K. Wu, S.S. Ng, et al., J. Control. Release 148 (2010) 292–302.
[10] A. Khoo, L.Y. Liu, J.O. Nyalwidhe, et al., Nat. Rev. Urol. 18 (2021) 707–724.
[11] K. Rasuleva, S. Elamurugan, A. Bauer, et al., ACS Sens. 6 (2021) 4489–4498.
[12] T. Katsila, A.P. Siskos, C. Tamvakopoulos, Mass. Spectrom. Rev. 31 (2012) 110–133.
[13] M. Vaudel, A. Sickmann, L Martens, Proteomics 10 (2010) 650–670.
[14] L. Zhang, J.E. Elias, Methods Mol. Biol. 1550 (2017) 185–198.
[15] J. Shi, J.M. Wong, J. Ma, et al., Bioanalysis 9 (2017) 251–264.
[16] M. Rauh, J. Chromatogr. B 883-884 (2012) 59–67.
[17] T. Gangnus, B.B. Burckhardt, Talanta 218 (2020) 121134.
[18] P.L. Bonate, D. Beyerlein, J. Crawford, et al., AAPS J. 9 (2007) 45.
[19] H. Tomioka, H. Nakagami, T. Sano, et al., Immunol. Endocrin. Metabol. Agent. Med. Chem. 14 (2014) 26–31.
[20] A. Millet, N. Khoudour, P. Bros, et al., Talanta 224 (2021) 121889.
[21] Z. Liu, B.D. Gray, C. Barber, et al., J. Control. Release 239 (2016) 223–230.
[22] M. Lisovsky, K. Patel, K. Cymes, et al., Arch. Pathol. Lab. Med. 8 (2007) 1304–1311.
[23] F.P. Carneiro, L.N.Z. Ramalho, S. Britto-Garcia, A. Ribeiro-Silva, S. Zucoloto, Dis. Colon. Rectum. 49 (2006) 588–594.
[24] M. Mehrpouya, Z. Pourhashem, N. Yardehnavi, M. Oladnabi, J. Cell. Physiol. 12 (2019) 21425–21435.